

Response of two-way reinforced concrete voided slabs enhanced by steel fibers and GFRP sheets under monotonic loading

Adel A. Al-Azzawi* and Shahad H. Mtashar^a

Department of Civil Engineering, College of Engineering, Al-Nahrain University, Jadriya, Baghdad, Iraq

(Received January 3, 2023, Revised March 8, 2023, Accepted March 12, 2023)

Abstract. Various efforts have been made to reduce the weight of concrete slabs while preserving their flexural strength. This will result in reducing deflection and allows the utilization of longer spans. The top zone of the slab requires concrete to create the compression block for flexural strength, and the tension zone needs concrete to join with reinforcing for flexural strength. Also, the top and bottom slab faces must be linked to transmit stresses. Voided slab systems were and are still used to make long-span slab buildings lighter. Eight slab specimens of (1000*1000 mm²) were cast and tested as two-way simply supported slabs in this research. The tested specimens consist of one solid slab and seven voided slabs with the following variables (type of slab solid and voided), thickness of slab (100 and 125 mm), presence of steel fibers (0% and 1%), and the number of GFRP layers). The voids in slabs were made using high-density polystyrene of dimensions (200*200*50 mm) with a central hole of dimensions (50*50*50 mm) at the ineffective concrete zones to give a reduction in weight by (34% to 38%). The slabs were tested as simply supported slabs under partial uniform loading. The results of specimens subjected to monotonic loading show that the combined strengthening by steel fibers and GFRP sheets of the concrete specimen (V-125-2GF-1%) shows the least deflection, deflection (4.6 mm), good ultimate loading capacity (192 MPa), large stiffness at cracking and at ultimate (57 and 41.74) respectively, more ductility (1.44), and high energy absorption (1344.83 kN.mm); so it's the best specimen that can be used as a voided slab under this type of loading.

Keywords: flexural behavior; monotonic loading; SSC; two-way voided slab; weight reduction

1. Introduction

The member used in the construction of floors, roofs, and bridge decks is known as a reinforced concrete slab. A building's floor system may consist of precast components, ribbed slabs, or in-situ solid slabs. Slabs may span in one or two directions and be supported by concrete or steel beams, walls, or the structure's columns directly (Alfeehan *et al.* 2017, Al-Azzawi and Abed 2017, Al- Al-Gasham *et al.* 2019, Yaagoob and Harba 2020, Al-Fakher *et al.* 2021, Al- Al-Gasham *et al.* 2021, Al-Azzawi and Shallal 2021, Pawar *et al.* 2022).

The slab, which consumes the most concrete quantity generally, is a major structural

*Corresponding author, Assistant Professor, E-mail: dr_adel_azzawi@yahoo.com

^aPh.D. Student, E-mail: shahadhameed91@gmail.com

component of building structures. Generally speaking, the slab is only designed to withstand the vertical load. Moreover, when the span of the building increases, the slab thickness would be increased and which leads to increasing column and foundation size which decrease the value of deflection of concrete and steel and this will lead to increasing cost (Senthil *et al.* 2018, Najm *et al.* 2019).

Various efforts have been made to reduce the weight of concrete slabs while preserving their flexural strength (Al-Azzawi and Al-Asdi 2017). This will result in reducing deflection and allows utilizing longer spans. The top zone of the slab requires concrete to create the compression block for flexural strength, and the tension zone needs concrete to join with reinforcing for flexural strength. Also, the top and bottom slab faces must be linked to transmit stresses. Bubble, waffle, hollow core, and beam-block slab systems were and are still used to make long-span slab buildings lighter.

During their service life, concrete members may need strengthening and maintenance. Design or construction problems, functional modifications, design code updates, lack of maintenance, change in the structural system, higher traffic volumes, blasts and explosions, and damage accumulated over time or caused by unexpected overloading, fires, or earthquakes may create this necessity. Because replacing weak structures demands enormous expenditures, strengthening has become the best approach to improve their load-bearing capacity and service life. While total replacement of a deficient/deteriorated element is preferable, strengthening/repair is sometimes more inexpensive and civil engineering infrastructure renewal has garnered substantial attention in recent years worldwide (Heiza *et al.* 2014).

Many researchers around the world study the effect of adding steel fibers to concrete slabs, the effect of reducing the slab weight, and the significant effect of strengthening the slabs by FRP sheets. (Baarimah and Syed Mohsin 2017) evaluated the potential impact of adding steel fiber to reinforced concrete slabs during a four-point bending test. (Ananda *et al.* 2019) studied the effect of the addition of different types of steel fibers with different contents on the width of cracks on the one-way slab under two-point loading.

Chung *et al.* (2018) analyzed the possibility of applying a donut-type two-way voided slab, which was investigated with a 12-point two-way bending test focused on global behaviors, including its load-bearing capacity, flexural stiffness, ductility, deflection, and load distribution by comparing the results with those of a solid slab with same properties. In 2019, Al kulabi and Al zahid investigated how dynamic loads affected the flexural capacity, serviceability loads, and failure type of RPC slabs. Three concrete slabs with steel fiber concentrations of 0, 1, and 2% underwent experimental testing. The results of the tests demonstrated that the steel fiber content is crucial in determining the static capacity of concrete slabs after they have been dynamically loaded. Increasing the steel fiber content improved the static loading capacity while also reducing the number and width of cracks and creating a safer environment for the occupants of the buildings.

Yadav *et al.* (2019) made a comparative study of a One-way bubble deck slab (770 mm*380 mm*110 mm) using the High-Density Polyethylene balls (70 mm diameter) of size prepared which is made up of plastic waste and conventional slab under cost analysis, load bearing capacity. All the previous research showed encouraging results which leads to the development of economical and effective systems in terms of structural behavior compared to solid slab traditional slab systems. Ayash, Abd-Elrahman, and Soliman (2020) studied the experimental and numerical performance of GFRP-repaired or strengthened reinforced concrete cantilever slabs..

In 2021, Abishek and Iyappan studied the flexural behavior of a bubble-deck slab strengthened with FRP, three slabs of (700 ×300×125 mm) were taken and tested under two points loading The

Table 1 Experimental specimen and parameters details

Slab Coding	Type of Slab	Thickness (mm)	% of Steel Fibers	No. of GFRP Layers
S-125-M	Solid	125	/	/
V-125-M	Voided	125	/	/
V-100-M	Voided	100	/	/
V-125-1GF-M	Voided	125	/	1
V-125-2GF-M	Voided	125	/	2
V-125-1%-M	Voided	125	1	/
V-125-1%-2GF-M	Voided	125	1	2
V-100-1%-2GF-M	Voided	100	1	2

bending behavior of a composite concrete slab roof with various techniques of external strengthening employing steel plates and carbon fiber reinforced polymer (CFRP) strips was studied by Najafi and Borzoo in 2022. Using numerical modeling, seven distinct models of square-shaped composite slab roofs are created in the ABAQUS program using finite element analysis. The concrete slab model, which has CFRP strips strengthened on its bottom surface, is first validated using experimental data.

All the previous research showed encouraging results which leads to the development of economical and effective systems in terms of the structural behavior of solid slab in traditional slab systems. Also, in the previous studies, voided slabs were investigated mainly as one-way or two-way thin slabs under concentrated impact or static loads. The strengthening technique used previously does not produce always a ductile failure due to the nature of used FRP materials. The present research investigates experimentally the behavior of two-way thin and moderately thick slabs cast with self-compacted concrete SCC and enhanced internally by steel fibers and externally by GFRP sheets under partial uniform static load. In general, the research challenge was if it is possible to produce strengthened moderately thick slabs that preserve a ductile flexural failure after strengthening with brittle material under static loading. The main task was to prevent the shear failure of these slabs which may happen due to the presence of voids in slabs. The voids will produce lighter slab components and therefore reduce the cost of foundations in low-bearing capacity soil regions.

2. Experimental work

2.1 Study parameters

Eight two-way slabs of square shape (1000*1000 mm) with variable thicknesses (125 and 100 mm) were cast and tested in the present work. The slabs were designed to fail in flexure using ACI 318 (2019) code. The main experimental parameters are the type of slab (solid or voided), slab thickness, number of GFRP sheet layers, presence of steel fibers, and type of loading. Details of these parameters and specimen codes are shown in Table 1. Each code of slab has many symbols such as Symbols (S, V) refer to the solid and voided slab, (M) refers to the monotonic loading, (1%) indicates the presence of steel fibers in concrete and (1GF, 2GF) represent the number of GFRP layers.

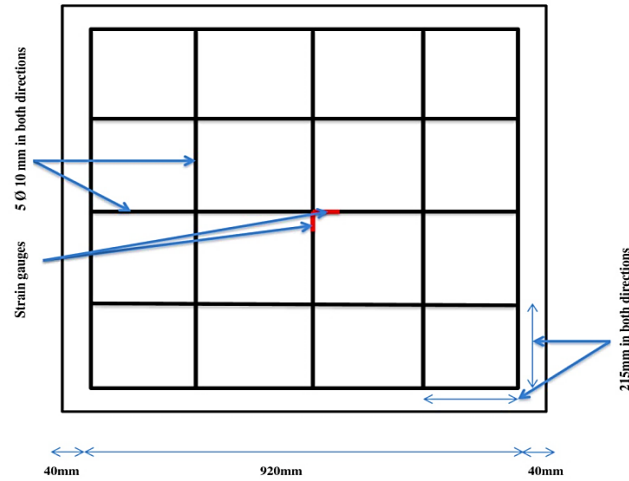


Fig. 1 Steel reinforcement details

2.2 Slab reinforcement details

Deformed steel bars of (10 mm) diameter were used. The bars were tied by steel wire as a mesh with openings of (215 mm) in both directions as shown in Fig. 1. Two strain gauges were fixed at the center of the middle reinforcing bars in both directions for the tested slab. The strain gauges used are FLAB-type (FLAB-6-11). Before the strain gauges are attached to the surface of the rebar, each reinforcing rebar's surface is first smoothed by removing the deformed ribs and cleaning them. The strain gauges are covered with water-resistant tape to protect them from the action of the materials during concrete placement and to avoid moisture absorption.

2.3 Biaxial voided blocks

The biaxial voided blocks used in this investigation were made with high-density polystyrene of dimensions (200*200*50 mm) with a central hole of dimensions (50*50*50 mm) to ensure and increase interaction between concrete, voids, and steel reinforcement. The distance between the voids was set to be 15 mm in both the longitudinal and transverse directions. The material used does not react with the concrete or the reinforcement; it has no porosity and has enough rigidity and strength to take over the loads when exposed to the wet concrete pouring process as shown in Fig. 2.

2.4 GFRP sheets strengthening system

Woven glass fiber is used with the epoxy-impregnating resin Sikadur-330 which consists of two components (A: Resin part and B: Hardener) as shown in Fig. 3. In this study, applying the glass fiber strips to the bottom face of the slab is done where the strips of dimensions (100 mm width and 700 mm length) and spaced by (100 mm) in both directions divided into four strips vertically and four strips glued horizontally in one layer for one specimen and two layers of strips for the other specimens.

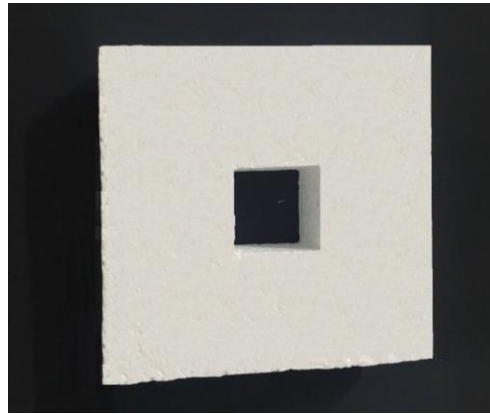


Fig. 2 Sample of voided block



Fig. 3 Sample of GFRP sheet and Epoxy resin Sikadur-330

Table 2 Concrete mix proportions

Mix	Silica	Gravel Kg/m ³	Sand	Steel	W/P	Water	S.P		
Name	Total binder Kg/m ³	(15% by wt. of binder) Cement Kg/m ³	Kg/m ³	fibers Kg/m ³		L/m ³	(1.5% by wt. of binder) lit/m ³		
M1	500	75	425	600	900	0	0.35	175	6.8
M2	500	75	425	600	900	78	0.35	175	6.8

2.5 Material

The concrete mixture is made in accordance with (EFNARC 2005) guidelines to achieve both the fresh and hardened characteristics of self-compacted concrete (SCC). Many mixed proportions were tried in this investigation to get the required compressive strength (Al-Azzawi and Al-Azzawi 2020). Two mixes (M1&M2) are considered and used in this investigation with different percentages of micro steel fibers (0 and 1%) as shown in Table 2.

Table 3 Fresh concrete characteristics

Test Method	Results (M1) 0% S.F	Results (M2) 1% S.F	EFNARC limits	
			Minimum	Maximum
Slump Flow (mm)	680	722	650	800
T500 (sec)	2.8	3.5	2	5
L-Box	0.83	0.88	0.8	1
U-Box (mm)	26	23	0	30
V- funnel (sec)	8	10	8	12

Table 4 Hardened concrete characteristics

Mix Name	f_{cu} MPa	f'_c MPa	f_t MPa	f_r MPa
M1	48.46	42.9	4.05	4.5
M2	63.07	57.4	6.6	7.3

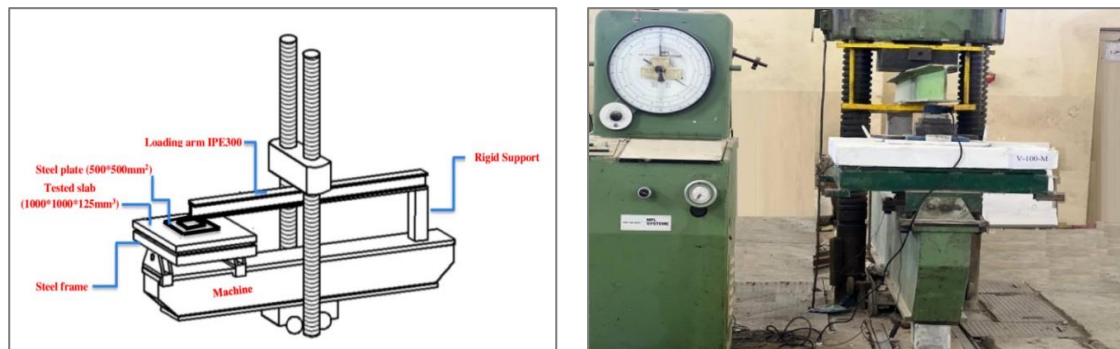


Fig. 4 Test setup

The workability test results obtained from the experimental work are compared with the limitations of (EFNARC 2005) which are related to fresh and hardened self-compacting concrete tests. The results of (Slump Flow and (T500), L-Box, U-Box, and V- funnel) tests for both mixes (M1&M2) are given in Table 3.

The test results of hardened SCC shown in Table 4 are the average of three specimens tested after (28) days of curing to specify their compressive strength (f_{cu} and f'_c) for cubs and cylinders respectively, splitting tensile strength (f_t) and flexural strength (f_r) for both mixes (M1&M2).

2.6 Test setup

All slabs are tested as a simply supported slab at all four edges by using a Hydraulically Universal Testing Machine of (3000 kN) capacity under static loads up to failure at the Structural Laboratory of the Faculty of Engineering, Al-Mustansiriyah University. The load is applied through a special steel frame as shown in Fig. 4. The frame is consisting of two parts; a loading arm and a supporting frame. The loading arm consists of a steel section of IPE300, the supporting frame consist of four C100 welded together to get rigid support, steel rod of diameter (25) mm

Table 5 Experimental results for slabs under monotonic loading

Slab Coding	First Cracking Load (Pcr) kN	Deflection at Cracking Load (Δ_{cr}) mm	Ultimate Load (Pu) kN	Deflection at Ultimate Load (Δ_u) mm
S-125-M	93	2.4	210	6.3
V-125-M	75	3	160	9.1
V-100-M	75	4.2	132	9.7
V-125-1GF-M	86	3.2	168	7.1
V-125-2GF-M	129	4	179	6
V-125-1%-M	99	2.5	183	5.7
V-125-1%-2GF-M	120	2.1	192	4.6
V-100-1%-2GF-M	100	3.3	183	6.8

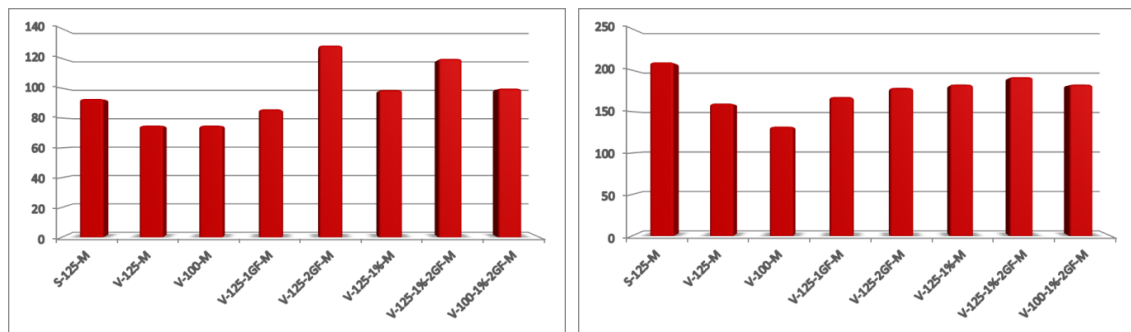


Fig. 5 First cracking and ultimate load for slabs

welded at the top of the frame to achieve roller boundary conditions. The load transfer from the machine to the specimens by the loading arm through a set of plates starting with (500*500 mm²), (300*300 mm²), (150*150 mm²), and two plates of (100*100 mm²) to ensure that the load will be distributed as a partial uniformly distributed load on the central area (500*500 mm²) of the specimens. A load cell of (50 tons) capacity is added beneath the loading arm to ensure the accuracy of loading. The deflection is measured by using (LVDT) at the center of the bottom face of each slab.

2.7 Experimental results of slabs under monotonic loading

Eight SCC slabs were tested under partial uniform monotonic loading until failure, one is solid and the others are voided slabs with the following variables:

- 1- Nature of the slab section (solid–voided)
- 2- Thickness of slab (thin and moderately thick)
- 3- No. of GFRP layers (1 layer – 2 layers)
- 4- Steel fibers existence (0%-1%)

2.7.1 Load-deflection relationship

Ultimate loads and cracking loads were recorded from the load cell as well as the deflections at cracking and deflections at ultimate were recorded by using (LVDT) at the center of the bottom face of the solid and voided slabs at a constant load step (each 5 kN). In general, for all concrete slabs, the deflection at ultimate load decreases when the slab thickness increases and steel fibers are added also, strengthening with GFRP sheets shows a remarkable reduction in deflection. The effect of different variables is divided into four categories depending on the (voids, thickness, No. of GFRP layers, and presence of steel fibers) on deflection and will be explained in detail below. The test results for slabs under monotonic loading are shown in Table 5 and Figs. 4 and 5. Load-deflection relationships for all specimens under monotonic loading are shown in Fig. 6 to Fig. 11.

2.7.1.1 Effect of voids

The effect of voids is shown clearly in the slab (V-125-M) compared to the solid slab (S-125-M) of the same dimensions and concrete mix as shown in Fig. 6. The solid slab exhibits an increase in ultimate load capacity by (24%) compared to voided slab while the deflection decreased by (44.5%)

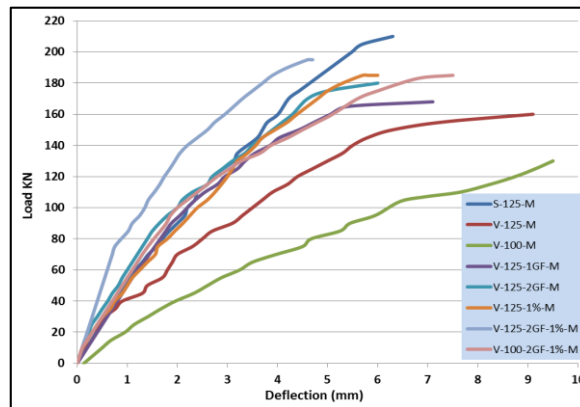


Fig. 6 Load-deflection relationship for slabs under monotonic loads

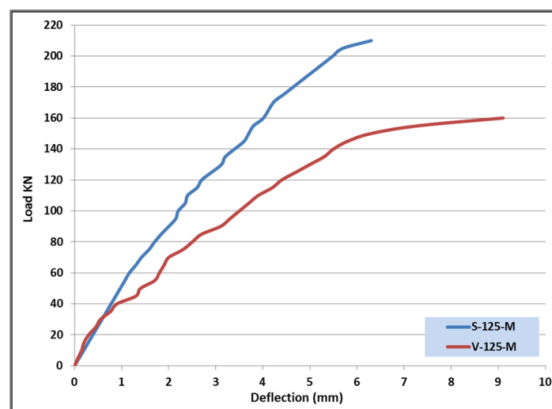


Fig. 7 Load- deflection relationship for (S-125-M & V-125-M)

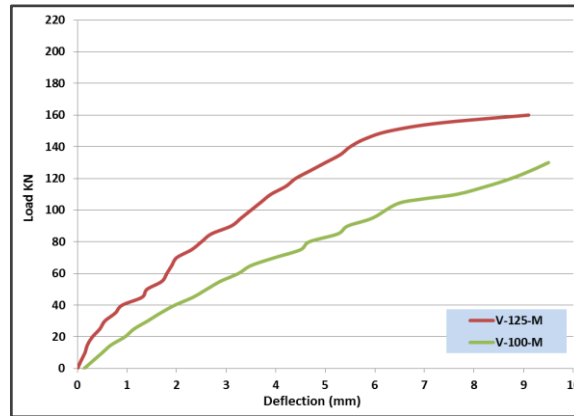


Fig. 8 Load- deflection relationship for (V-125-M & V-100-M)

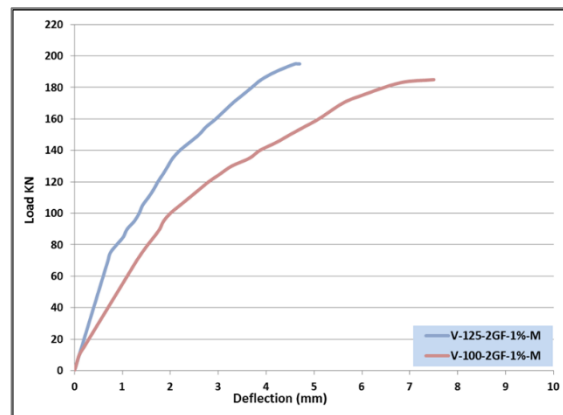


Fig. 9 Load- deflection relationship for (V-125-2GF-1%-M & V-100-2GF-1%-M)

at the same stage of loading. This variation in percentages of load capacity and deflection was expected due to a contribution of concrete with a large cross-sectional area under the neutral axis to resist the tensile stresses in contrast to the less cross-sectional area under the neutral axis for the voided slab. The percentage of the deflection at cracking to that at ultimate stages ranged from (67% to 62%) for voided and solid slabs respectively. This value was influenced by the magnitude of reduction in cross-sectional area due to the reduction in the weight of voided slab which is equal to (34.8%) of the weight of the solid slab which means less amount of concrete and more deflection.

2.7.1.2 Effect of thickness

In general, when the thickness of the slab increased from (100 to 125 mm), the first cracking and the ultimate load increased in strengthened voided slabs (V-100-M, V-125-M) and strengthened slabs (V-100-2GF-1%-M) with (V-125-2GF-1%-M).

The increase in thickness from 100 to 125 mm resulted in an improvement in the ultimate load capacity for the voided slabs without strengthening by (17.5%) while the deflection was reduced by (7%) compared to slab (V-100-M) at the same stage of loading as shown Fig. 7.

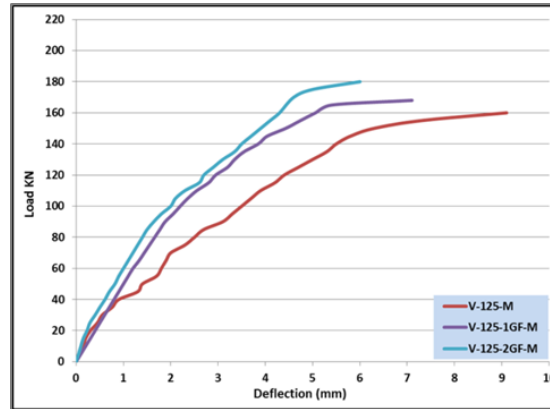


Fig. 10 Load- deflection relationship for (V-125-M, V-125-1GF-M & V-125-2GF-M)

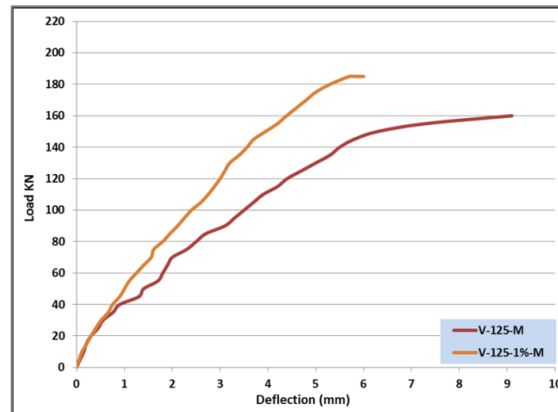


Fig. 11 Load- deflection relationship for (V-125-M & V-125-1%M)

Also, the increase in thickness from 100 to 125 mm in strengthened voided slabs lead to an increase in the ultimate load capacity for slab by only (4%) where the deflection decreased by (47.8%) compared to slab (V-100-2GF-1%-M) as shown in Fig. 8.

This decrease in deflection for specimens of (125 mm) thickness can be attributed to that when the thickness is decreased to (100 mm); the flexural rigidity decreases and this means less stiffness which leads to a significant increase in deflection values in comparison to specimens of (125 mm) thickness and this effect the first and ultimate loading cracks with increasing loading stages.

It can be seen that the increase in the thickness to 125 mm for strengthened slabs is very efficient in deflection where the value of deflection of strengthened voided slabs decreased remarkably up to (50%) compared to the value of unstrengthened ones. This is attributed to the presence of steel fibers which prevents the cracks from growing and expanding also the bonding of GFRP sheets prevents or surrounding cracks and results in decreasing the deflection in a wide range.

2.7.1.3 Effect of GFRP layers

Strengthening slabs by GFRP sheets with one layer or two layers at the bottom face of concrete

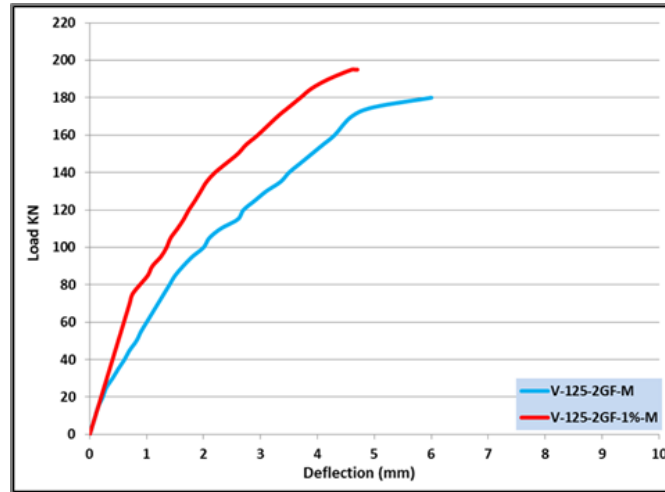


Fig. 12 Load-deflection relationship for (V-125-2GF-1%-M & V-125-2GF-M)

specimens shows a good influence on decreasing the deflection at cracking and ultimate stages.

Voided slab (V-125-1GF-M) which strengthened with one layer of GFRP sheet shows a little increase in ultimate capacity by (5%) while the decrease in deflection reaches (28.2%) compared to the specimen (V-125-M) as shown in Fig. 9.

As shown in Fig. 9, voided slab (V-125-2GF-M) which strengthened with two layers of GFRP sheet has an increase in ultimate capacity by (10.6%) while the deflection decreased by (52%) as compared to the specimen without strengthening (V-125-M). A comparison between one layer and two layers of GFRP sheets of strengthened specimens shows an increase in ultimate capacity by (6.2%) and a decrease in deflection by (18.33%) for (V-125-2GF-M) as compared to (V-125-1GF-M).

It can be seen that the increase in ultimate load capacity under the effect of strengthening by GFRP sheets is increased as the number of sheets increased and this increase is considered a little as compared to the decrease in deflection and this is due to restriction of the cracks propagation by GFRP sheets which increase the stiffness and rigidity of slabs. This will be increased as the number of GFRP layers increases.

2.7.1.4 Effect of steel fibers

In general, the relationship between the load and deflection of steel fiber concrete is an extrusive relation and it is found that the deflection is decreased.

At the same stage of loading, the effect of adding steel fibers by (1%) for voided slab without GFRP strengthening (V-125-1%- M) lead to an increase in the ultimate load capacity for slab by (12.6%) and the deflection is decreased by (60%) compared to slab (V-125-M) as shown in Fig. 10.

For GFRP strengthening voided slab (V-125-2GF-1%-M), adding the steel fibers increased the ultimate load capacity by (6.8%) and the deflection decreased by (30.4%) compared to slab (V-125-2GF-M) as shown in Fig. 11.

The increase in the first and ultimate loading cracks with increasing loading stages by the addition of steel fibers restricts the growth and expansion of cracks, transfers tensile stress to the concrete and surrounding cracks, and increases the load capacity.

Table 6 Cracking and ultimate stiffness for slabs under monotonic loading

Slab Coding	P _{cr} kN	Δ _{cr} mm	K _{cr} KN/mm	P _u kN	Δ _u mm	K _u KN/mm
S-125-M	93	2.4	38.75	210	6.3	33.33
V-125-M	75	3	25	160	9.1	17.6
V-100-M	75	4.2	17.86	132	9.7	13.6
V-125-1GF-M	86	3.2	26.87	168	7.1	23.66
V-125-2GF-M	129	4	32.25	179	6	29.8
V-125-1%-M	99	2.5	40	183	5.7	32
V-125-1%-2GF-M	120	2.1	57	192	4.6	41.74
V-100-1%-2GF-M	100	3.3	30.3	183	6.8	27

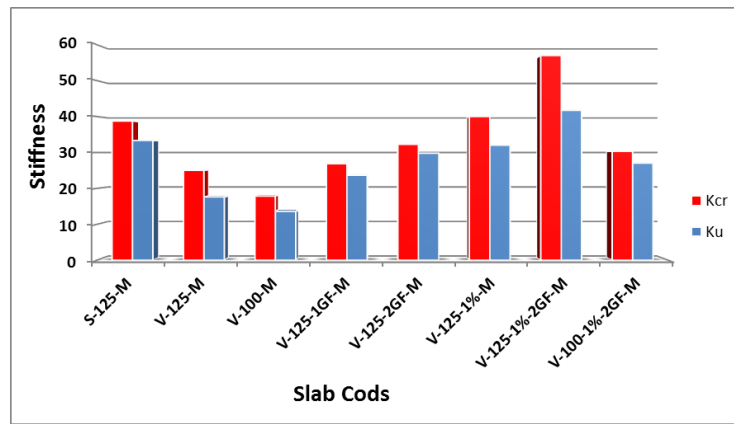


Fig. 13 Cracking and ultimate stiffness for slabs under monotonic loading

2.7.2 Flexural stiffness of slabs

Bending stiffness (or the load-deflection slope) is the resistance of a member against bending deformation. It depends on the elastic modulus E , the moment of inertia, member effective length, and boundary conditions. Secant stiffness was calculated using Eqs. (1(a) and 1(b)).

$$K = \frac{P_{cr}}{\Delta_{cr}} \quad (1a)$$

$$K = \frac{P_u}{\Delta_u} \quad (1b)$$

Table 6 shows the result for calculated secant stiffness (K) under cracking and ultimate stages.

In general, the stiffness decreased gradually during load application so it is noticed that all the values of (K_u) are smaller than (K_{cr}). This can be attributed to the appearance of cracks, lack of bonding between the concrete and steel bars, and increasing the number, width, and length of cracks through load application as shown in Fig. 12. The strengthened specimens exhibit much stiffer responses and lower deflections than the corresponding unstrengthened specimens.

At cracking and ultimate loading stages the secant stiffness increased in the solid section compared to the voided due to the reduction in the flexural rigidity and voids existence as well as increasing the slab thickness from (100 to 125 mm) leading to increasing (K_{cr} and K_u).

Table 7 Ductility index and energy absorption for slabs under monotonic loading

Slab Coding	Δu mm	Δy mm	$\mu d = \frac{\Delta u}{\Delta y}$	Energy Absorption (kN.mm)
S-125-M	6.3	5	1.26	836.75
V-125-M	9.1	7.8	1.17	705.9
V-100-M	9.7	8.5	1.14	700.82
V-125-1GF-M	7.1	5.8	1.22	889.83
V-125-2GF-M	6	4.5	1.33	1155.42
V-125-1%-M	5.7	4.2	1.36	1205.58
V-125-1%-2GF-M	4.6	3.2	1.44	1344.83
V-100-1%-2GF-M	6.8	5.5	1.24	897.68

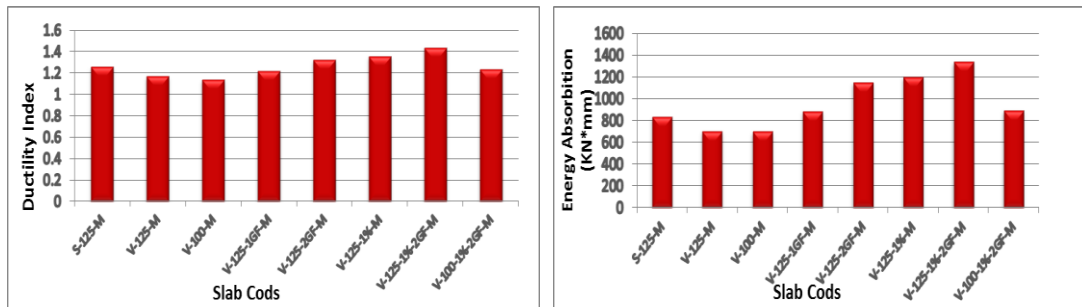


Fig. 14 Ductility index and energy absorption magnitude for slabs

Applying GFRP sheets to the tension face of specimens increase stiffness at cracking and ultimate loading stages by (16.7% and 20.6%) respectively for the two layers of GFRP compared to one layer due to increasing the rigidity and cracking resistance of the specimens.

Adding steel fibers to the mix for voided slab (V-125-1%-M) lead to an increase in the stiffness at cracking and ultimate stages by (37.5% and 45%) respectively. This may be due to the main function of the fibers which increase the tensile strength and manage cracks propagation leading to reduce concrete failure.

Strengthening slabs with both steel fibers and GFRP sheets shows the greatest values of stiffness at cracking and at ultimate (56% and 58%) respectively compared to the un-strengthening one.

It is can be concluded that the specimen (V-125-2GF-1%-M) is the batter one which has the largest cracking and ultimate stiffness (57 and 41.74) respectively. This can be attributed to the two enhancements (steel fibers and GFRP sheet) applied to it.

2.7.3 Ductility and energy absorption of slabs

Ductility and energy absorption are considered inseparable properties for reinforced concrete structures. Ductility is a desirable structural property because it allows forces redistribution and provides a warning of impending failure; therefore, it is a structural design requirement in most design codes. Energy absorption is equal to the area under the load-deflection curve or the area under the stress-strain curve (Al kulabi *et al.* 2019).

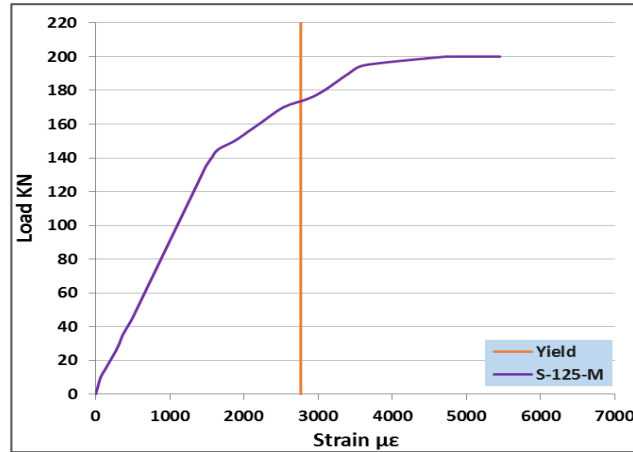


Fig. 15 Load-strain curve for (S-125-M)

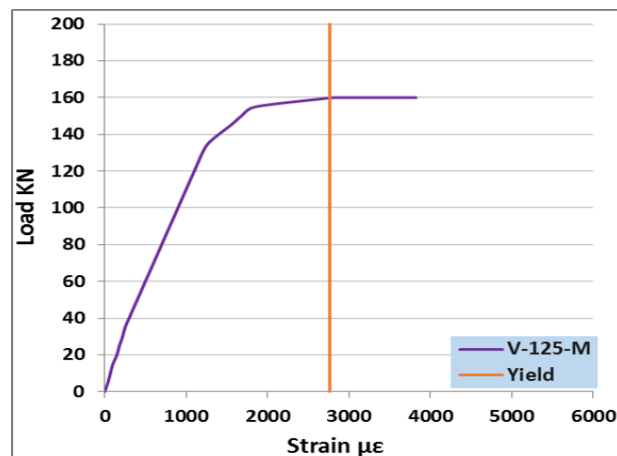


Fig. 16 Load-strain curve for (V-125-M)

There are two types of failure; ductile failure with prior notice before fracture and brittle failure which is characterized by the suddenness and uncontrolled nature. Ductile materials can absorb a great amount of energy before fracture, while brittle materials absorb a little amount (Kristombu Baduge *et al.* 2019). Table 7 and Fig. 13 show the ductility index and energy absorption magnitude for slabs under monotonic loading. The ductility index is considered as the ratio between the ultimate deflections of the slab to the deflection at steel reinforcement yielding. Energy absorption is calculated according to the trapezoidal rule from load-deflection curves through Eq. (2) by using an excel program.

$$T = \left(\frac{\Delta x}{2}\right) [f(x_0) + 2f(x_{1,2,3,\dots,n-1}) + f(x_n)] \quad (3)$$

Δx : variation in deflection values (values in X-axis)

$f(x)$: load values (Values in the y-axis)

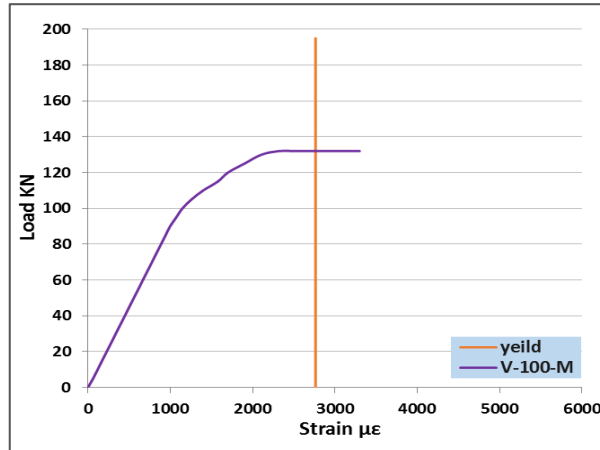


Fig. 17 Load-strain curve for (V-100-M)

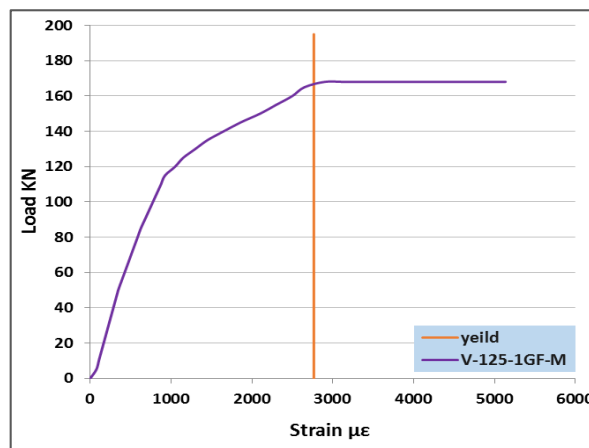


Fig. 18 Load-strain curve for (V-125-1GF-M)

All the strengthened voided specimens with steel fibers and GFRP strips have energy absorption and ductility greater than the unstrengthened specimens.

The presence of voids leads to a decrease the energy absorption and ductility by (15.64% and 7.14%) respectively compared to solid slab. This can be attributed to the fact that the removed concrete located below the neutral axis is not effective in increasing ductility. Increasing the thickness from (100 to 125 mm) gives an increase in ductility and energy approximately with similar values for both ductility and energy absorption compared to (V-100-M).

The addition of steel fibers to the concrete mixture increases the energy absorption and ductility of the tested specimen (V-125-1%-M) by (41.44% and 14%) respectively compared to the specimen without steel fibers (V-125-M), so the presence of steel fibers results in a more ductile type of failure.

Strengthening of slabs by GFRP sheets lead to improve energy absorption by (20.6% and 40%) while the ductility increased by (4% and 19%) for one and two layers respectively compared to (V-125-M).

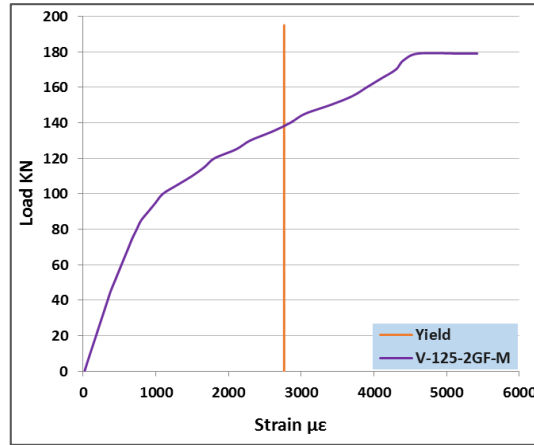


Fig. 19 Load-strain curve for (V-125-2GF-M)

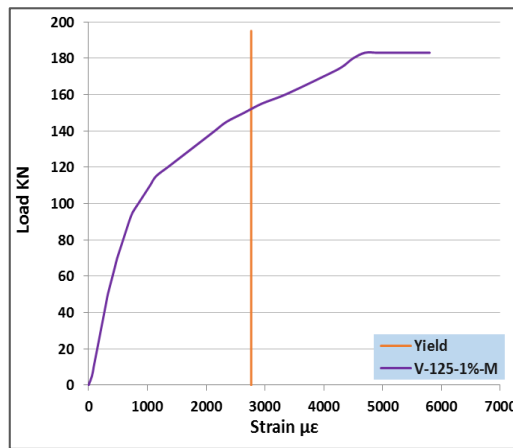


Fig. 20 Load-strain curve for (V-125-1%-M)

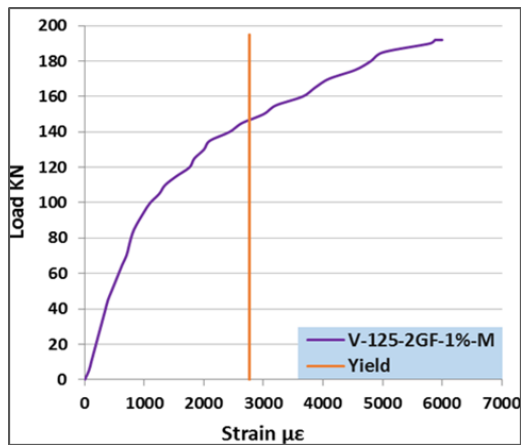


Fig. 21 Load-strain curve for (V-125-2GF-1%-M)

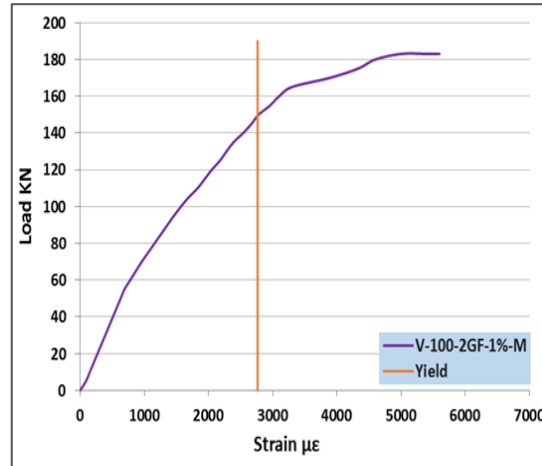


Fig. 22 Load-strain curve for (V-100-2GF-1%-M)

It can be noticed that the ductility and energy absorption of all specimens can be considered to be close except specimens strengthened with steel fibers and GFRP sheets (two layers) gives the highest percentage of energy absorption and ductility as seen in the specimen (V-125-2GF-1%-M) which can be considered as the better one.

2.7.4 Load-strain relationship

During the testing of reinforced concrete slabs, electrical strain gauges of type (FLAB-6-11) were attached to the reinforcing bars to record the strains in the steel. Central positions of main steel bars were chosen to evaluate the behavior of steel reinforcements. The load-strain relationships for steel reinforcement were computed and discussed depending on the variables taken in this study including the effect of (voids, thickness, no. of GFRP layers, and presence of steel fibers). The steel strain at yield is equal to (2765 µε) for Ø10 mm reinforcement. Load-strain curves for all specimens tested under monotonic loading are illustrated in Figs. 14 to 21.

2.7.4.1 Effect of voids

The effect of voids on steel strain can be seen clearly when making a comparison between (S-125-M) and (V-125-M) where at the early stages of loading, both specimens behave linearly and the developed strains are small. Further increase in loading leads to an increase in the strain of the solid slab by (30%) more than the voided slab due to the increase in the ultimate load of the solid slab as shown in Figs. 14 and 15.

2.7.4.2 Effect of thickness

Increasing the thickness from (100 to 125 mm) led to an increase in the ultimate loads and this increase was reflected in the strain of steel bars as shown in Figs. 15 and 16. At the early stages of loading, all specimens of this group behave linearly and the developed strains are gradual. Further increase in loading leads to an increase in the strain by (13.7%) of the slab (V-125-M) compared to (V-100-M) while the increase in strain for strengthening slabs (V-125-2GF-1%-M) and (V-100-2GF-1%-M) is only (6.67%) as shown in Figs. 20 and 21. This may be due to the presence of GFRP sheets and steel fibers which compensate for the effect of decreasing the thickness.

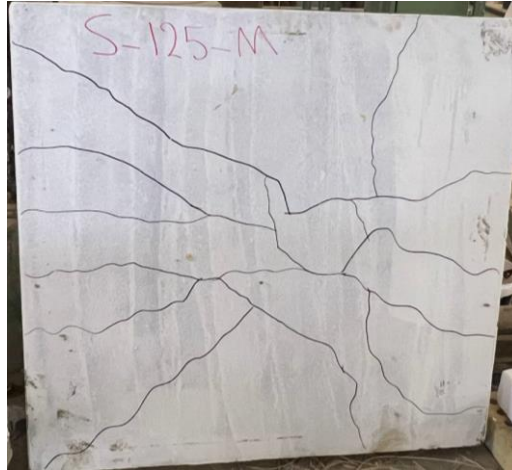


Fig. 23 Failure pattern of (S-125-M)



Fig. 24 Failure pattern of (V-125-M)

2.7.4.3 Effect of GFRP layers

This group showed that the strengthening with GFRP sheets lead to improving the strain of bottom steel bars. The strain of strengthening slabs by one and two layers increased by (25.5% and 29.4%) respectively compared to (V-125-M) as shown in Figs. 15, 17, and 18. This means that the strengthening with two layers of GFRP sheets affects the strain due to the high ultimate load of (V-125-2GF-M) compared to (V-125-1GF-M).

2.7.4.4 Effect of steel fibers

The addition of steel fibers increases the tensile strength of overall slabs as well as increase ductility. This group shows the effect of adding steel fibers to the mix, so the increase in the strain of slabs (V-125-1%-M and V-125-2GF-1%-M) are (34% and 10%) compared to (V-125-M and V-125-2GF-M) respectively as shown in Figs. 15, 18, 19 and 20. This may be due to the high



Fig. 25 Failure pattern of (V-100-M)



Fig. 26 Failure pattern of (V-125-1GF-M)

ultimate loads of these slabs compared to non-fibrous specimens. Finally, it can be concluded that the steel strain increases as the ultimate load increases and when the slabs enhance internally by steel fibers or externally by GFRP sheets or both of them.

2.7.5 Cracking pattern and mode of failure for slabs under monotonic loading

At the early stages of load application, the specimens show high stiffness and high resistance to loads until the appearance of the first crack. The development of cracking gives helpful information concerning the mechanism of failure mode.

For all specimens, the first crack was observed at the middle distance between supports on the bottom face of the slab, and then as the applied load is increased, cracks propagated towards the load point resulting in a flexural failure as shown in Figs. 22 to 29. The width and size of cracks



Fig. 27 Failure pattern of (V-125-2GF-M)



Fig. 28 Failure pattern of (V-125-1%-M)



Fig. 29 Failure pattern of (V-125-2GF-1%-M)



Fig. 30 Failure pattern of (V-100-2GF-1%-M)

are much lesser in slabs strengthening with steel fibers due to the capability of steel fibers to arrest the crack development and thus minimize the size of the damaged area as well the strengthening by GFRP sheets delays the cracks initiation and arrested their propagation and control tension crack growth by the confining concrete.

The failure mode of all specimens is "flexural failure" but the crack pattern is different from one slab to another due to using different variables like (steel fibers which arrest the crack development and thus minimize the size of the damaged area as well the strengthen by GFRP sheets delays the cracks initiation and arrested their propagation and control tension crack growth by the confining concrete).

3. Conclusions

The main conclusions drawn from this research are:

- The presence of voids in two-way slabs reduces the weight by (34% to 38%) for moderately thick and thin slabs respectively and thus minimizes material used, reduction of construction, lower cost, green technology etc. This would be reflecting mainly on the size of foundations.
- To improve the overall performance of slab without increasing the cost and maintain the ductile behavior, using GFRP sheets is the suitable chose under static loading. Using steel fibers compensating their poor rigidity and stiffness.
- Increasing the thickness from (100 to 125 mm) led to an increase in the ultimate load capacity by (17.5%) and decreasing the deflection by (7%) for unstrengthen slabs while the same comparison was made for strengthened slabs and found that the ultimate capacity increased by (4%) and decreasing the deflection by (47.8%) and this may be due to the presence of steel fibers which prevents the cracks from growing and expanding also the bonding of GFRP sheets prevents or surrounding cracks and results in decreasing the deflection in a wide range.

- Strengthening slabs by GFRP sheets with one layer or two layers at the bottom face of concrete specimens shows a good influence on decreasing the deflection up to (52%) for two layers of GFRP sheets.
- At the same stage of loading, the effect of adding steel fibers by (1%) for voided slab) lead to a decrease the deflection by (60%). This may be due to the action of steel fibers which restricts the growth and expansion of cracks, transfers tensile stress to the concrete and surrounding cracks, and increases the load capacity.
- It is can be concluded that the specimen (V-125-2GF-1%-M) is the batter one which has the largest cracking and ultimate stiffness (57 and 41.74) respectively. This can be attributed to the two enhancements (steel fibers and GFRP sheet) applied to it.
- It can be noticed that the ductility and energy absorption of all specimens can be considered to be close except specimens strengthened with steel fibers and GFRP sheets (two layers) gives the highest percentage of energy absorption and ductility as seen in the specimen (V-125-2GF-1%-M) which can be considered as the batter one.

References

- Abishek, V. and. Iyappan, G.R (2021), "Study on flexural behavior of bubble deck slab strengthened with FRP", *J. Phys.: Conference Series*, 2040(2021), <https://doi.org/10.1088/1742-6596/2040/1/012018>.
- ACI 318 (2019), Building code requirements for structural concrete and commentary, American Concrete Institute, Farmington Hills, Michigan.
- Adil, A.I., Hejazi, F. and Rashid, R.S.M. (2019), "Voided biaxial slabs - state of art", In *IOP Conference Series: Earth and Environmental Science*. 357. Institute of Physics Publishing.
- Al-Azzawi, A.A. and Al-Asdi, A.J. (2017), "Behavior of one way reinforced concrete slabs with styropor blocks", *Adv. Concrete Constr.*, **5**(5), 451-468. <https://doi.org/10.12989/acc.2017.5.5.451>.
- Al-Azzawi, A.A. and Abed, S.A. (2017), "Investigation of the behavior of reinforced concrete hollow-core thick slabs", *Comput. Concrete*, **19**(5), 567-577. <https://doi.org/10.12989/cac.2017.19.5.567>.
- Al-Azzawi, A.A. and Shallal, M.S. (2021), "Behavior of reinforced sustainable concrete hollow-core slabs", *Adv. Concrete Constr.*, **11**(4), 271-284. <https://doi.org/10.12989/acc.2021.11.4.271>.
- Al-Fakher, U., Manalo, A., Ferdous, W., Aravinthan, T.H., Zhuge, Y., Bai, Y. and Edoo, A. (2021), "Bending behaviour of precast concrete slab with externally flanged hollow FRP tubes", *Eng. Struct.*, **241**. <https://doi.org/10.1016/j.engstruct.2021.112433>.
- Al-Gasham, T.S., Hilo, A.N. and Alawsi, M.A. (2019), "Structural behavior of reinforced concrete one-way slabs voided by polystyrene balls", *Case Studies in Constr. Mater.*, **11**. <https://doi.org/10.1016/j.cscm.2019.e00292>
- Al-Gasham, T.S., Mhalhal, J. and Abid, S.R. (2021), "Quasi-static analysis of biaxial voided slabs with openings", *Structures*, **33**, 4176-4192. <https://doi.org/10.1016/j.istruc.2021.07.021>.
- Alfeehan, A., Abdulkareem, H. and Mutashar, S. (2017), "Flexural behavior of sustainable reactive powder concrete bubbled slab flooring elements", *Challenge J. Struct. Mech.*, **3**(2), 81. <https://doi.org/10.20528/cjsmec.2017.04.010>.
- Al kulabi, A.K. and Al zahid, A.A. (2019), "Influence of dynamic loading induced by free fall ball on high-performance concrete slabs with different steel fiber contents", *Struct. Monit. Maint.*, **6**(1), 19-32. <https://doi.org/10.12989/smm.2019.6.1.019>.
- Ananda, F., Febriani, O., Pribadi, J.A., Junaidi, J. and Gunawan, S. (2019), "Effect the use of steel fibers (Dramix) on reinforced concrete slab", *CSID J. Infrastruct. Develop.*, **2**(2), 183. <https://doi.org/10.32783/csidi-jid.v2i2.52>.
- Ayash, N.M., Abd-Elrahman, A.M. and Soliman, A.E. (2020), "Repairing and strengthening of reinforced concrete cantilever slabs using glass fiber-reinforced polymer (GFRP) wraps", *Structures*, **28**, 2488-2506.

- <https://doi.org/10.1016/j.istruc.2020.10.053>.
- Baarimah, A.O. and Mohsin, S.M.S. (2017), "Behaviour of reinforced concrete slabs with steel fibers", *In IOP Conference Series: Materials Science and Engineering*, 271. Institute of Physics Publishing.
- Chung, J.H., Jung, H.S., Bae, B., Choi, C.H. and Choi, H.K. (2018), "Two-way flexural behavior of donut-type voided slabs", *Int. J. Concrete Struct. Mater.*, **12**. <https://doi.org/10.1186/s40069-018-0247->
- Chung, J.H., Bae, B., Choi, H.K., Jung, H. and Choi, C.H. (2018), "Evaluation of punching shear strength of voided slabs considering the effect of the ratio b_0/d ", *Eng. Struct.*, **164**, 70-81, <https://doi.org/10.1016/j.engstruct.2018.02.085>.
- Gil-Martin, L.M. and Hernandez-Montes, E.(2021),"Review of the reinforcement sizing in the strength design of reinforced concrete slabs", *Comput. Concrete*, 27(3):211-223, <https://doi.org/10.12989/cac.2021.27.3.211>
- Khalid Heiza, A.K., Meleka, N. and Tayel, M. (2014). "State-of-the art review: Strengthening of reinforced concrete structures–different strengthening techniques", *Proceedings of the International Conference on Nano-Technology in constructions*, 1, March.
- Kristombu Baduge, S., Mendis, P., Ngo, T.D. and Sofi, M. (2019), "Ductility design of reinforced very-high strength concrete columns (100–150 MPa) using curvature and energy-based ductility indices", *Int. J. Concrete Struct. Mater.*, **13**(1). <https://doi.org/10.1186/s40069-019-0347-y>.
- Najafi, S. and Borzoo, S. (2022), "Different strengthening designs and material properties on bending behavior of externally reinforced concrete slab", *Struct. Monit. Maint.*, **9**(3), 271-287, <https://doi.org/10.12989/smm.2022.9.3.271>.
- Najm, I.N., Daud, R.A. and Al-Azzawi, A.A. (2019), "Behavior of reinforced concrete segmental hollow core slabs under monotonic and repeated loadings", *Struct. Monit. Maint.*, **6**(4), 269-289. <https://doi.org/10.12989/smm.2019.6.4.269>.
- Pawar, A.J., Mathew, N.S., Dhake, P.D. and Patil, Y.D. (2022), "Flexural behavior of two-way voided slab", *Mater. Today Proceedings*, **65**(2), 1534-1545. <https://doi.org/10.1016/j.matpr.2022.04.500>.
- Senthil, K., Shailja, B., Saurabh, J.K., Abhishek, R. and Tanzeem, A. (2018), "Study on influence of thickness and span length of flat slab for progressive collapse", *Proceedings of the National Conference : Advanced Structures, Materials And Methodology in Civil Engineering (ASMMCE – 2018)*, 3-4, November.
- Wang, L., He, T., Zhou, Y., Tang, S., Tan, J., Liu, Z. and Su, J. (2021), "The influence of fiber type and length on the cracking resistance, durability and pore structure of face slab concrete", *Constr. Build. Mater.*, **282**, 122706. <https://doi.org/10.1016/j.conbuildmat.2021.122706>.
- Yaagoob, A.H. and Harba, I.S. (2020), "Behavior of self compacting reinforced concrete one way bubble deck slab", *Al-Nahrain J. Eng. Sci.*, **23**(1), 11.
- Yadav, S., Sharif Uddin, M., Pal, V.K., Ahmed, Z. and Gupta, A. (2019), "An experimental study on bubble deck slab system with HDPE balls", *Int. J. Innov. Res. Technol.*, **5**(12).